# Accepted Manuscript

Research paper

Remarkable differences and similarities between the isomeric Mn(II)- *cis*- and *trans*-1,2-diaminocyclohexane-*N,N,N',N'* -tetraacetate complexes

Enikő Molnár, Balázs Váradi, Zoltán Garda, Richárd Botár, Ferenc K. Kálmán, Éva Tóth, Carlos Platas–Iglesias, Imre Tóth, Ernő Brücher, Gyula Tircsó
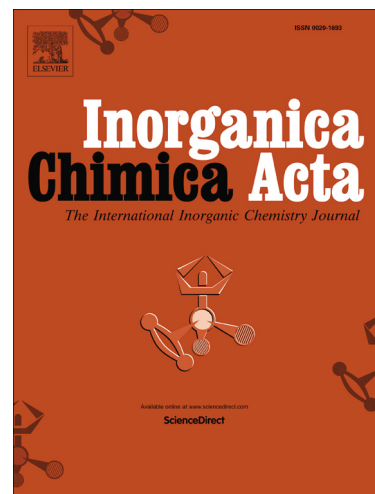
# Remarkable differences and similarities between the isomeric Mn(II)- *cis*- and *trans*-1,2-diaminocyclohexane-*N,N,N′,N′*-tetraacetate complexes

*Enikő Molnár[a], Balázs Váradi[a], Zoltán Garda[a], Richárd Botár[a,b], Ferenc K. Kálmán[a,b,c], Éva Tóth[b], Carlos Platas-Iglesias[d], Imre Tóth[a], Ernő Brücher[a] and Gyula Tircsó[a*]*

[a] Department of Inorganic and Analytical Chemistry, Faculty of Science and Technology, University of Debrecen, Debrecen, Egyetem tér 1, H-4010, Hungary

[b] Centre de Biophysique Moléculaire, CNRS, Université d'Orléans, rue Charles Sadron, 45071 Orléans, Cedex 2, France

[c] Le Studium, Loire Valley Institute for Advanced Studies, 1 Rue Dupanloup, 45000 Orléans, France

[d] Centro de Investigacións Científicas Avanzadas (CICA), Departamento de Química, Universidade da Coruña, Campus da Zapateira-Rúa da Fraga 10, A Coruña, Spain

This paper is dedicated to Prof. Imre Sóvágó on the occasion of his 70th birthday.

Corresponding author e-mail: gyula.tircso@science.unideb.hu

**Keywords**

**Abstract**

Equilibrium, kinetic (solvent exchange and dissociation of the complex) and relaxometric studies ($^1$H and $^{17}$O NMR) have been performed with the $[M(II)(c\text{-cdta})]^{2-}$ complexes ($c$-cdta = $cis$-1,2-diaminocyclohexane-$N,N,N',N'$-tetraacetic acid, M(II)= Mn(II), Zn(II), Cu(II),Ca(II), Mg(II)) and the physico-chemical data are compared to the isomeric complexes with $trans$-1,2-cdta ($t$-cdta) with the aim of searching appropriate ligands for Mn(II) complexation for safe MRI contrast agents. The total basicity ($\Sigma \log K_i^H$) of the $c$-cdta ligand appears to be very similar to that of the $trans$- derivative under the conditions applied (I=0.15 M NaCl and 25 $^o$C), but the first two protonation constants notably differ. $\log K_1^H$ is 1.5 log units higher, while the $\log K_2^H$ is 0.8 log units lower than those determined for the $trans$-derivative. Similar basicity of the ligands results in similar complex stability ($\log K_{[Mn(L)]}$ values are 14.19(2) and 14.32), whereas the conditional stabilities near to physiological pH are different (pMn values are 7.82 and 8.68) for the $[Mn(c\text{-cdta})]^{2-}$ and the $[Mn(t\text{-cdta})]^{2-}$ derivatives, respectively. Dissociation kinetic studies revealed that the $[Mn(c\text{-cdta})]^{2-}$ dissociates 250 times faster than the $[Mn(t\text{-cdta})]^{2-}$ complex. The water exchange rate ($k_{ex}^{298}$) of $[Mn(c\text{-cdta})]^{2-}$ is ca. 60% higher than that of $[Mn(t\text{-cdta})]^{2-}$. The differences can likely be attributed to the different distances between the individual donor atoms, and the arrangement of the donor atoms around the metal ions in the $cis$- and $trans$- isomers. Interestingly, the relaxivity values of the Mn(II) complexes are very close ($r_{1p}$ = 3.79 mM$^{-1}$s$^{-1}$ and 3.62 mM$^{-1}$s$^{-1}$; 20 MHz, 25 °C for the $cis$- and $trans$-isomers, respectively). DFT calculations were used to gain insight into the different properties of the $[Mn(c\text{-cdta})]^{2-}$ and the $[Mn(t\text{-cdta})]^{2-}$ complexes. The results gained in our studies confirm that the $trans$-1,2-cyclohexanediamine "building block" displays better features for further ligand development.

**Introduction**

The linear and macrocyclic aminopolycarboxylate (APC) complexes are widely used in medical diagnosis and therapy for the complexation of metal ions applied in the field of

nuclear medicine, optical and magnetic resonance imaging (MRI) [1-7]. These different fields have some special claims regarding the properties of complexes, but the general requirements, which should be accomplished for all the complexes, are the high stability and kinetic inertness. In other words, it means that the complexes must not dissociate in the body of patients during or after the examinations are performed. Considering the very complex nature of biological fluids which contain a great number of metal ions and complex forming ligands, this is a very strict requirement. To prevent any interaction between the APC complexes in use and the endogenous metals or ligands, the structure of APC ligands play very important role. So the ligands have to be specially designed for the robust complexation of metal ions. To design a ligand, the chemical properties of the metal ion, its ionic size, electronic structure and coordination number are considered first to find out how many and which kind of donor atoms are optimal for the complexation. Some special structural elements may also be beneficial e.g. the rigidity of the ligand and/or its degree of pre-organization to bind the metal ion, which can be achieved by the use of suitable functional group(s) and/or by introducing some cyclic or macrocyclic building blocks.

In MRI several Gd(III) – APC complexes are clinically used as contrast agents (CAs) to increase the contrast between the healthy and diseased tissues or organs by differently increasing the relaxation rates of protons (mainly water protons) in the body. The ligands used for metal ion complexation in CAs are the linear dtpa, the macrocyclic dota and their derivates [6, 7]. Nowadays there are 6 linear and 3 macrocyclic CAs in clinical use, but in the last decade some concerns arose with the use of the linear agents. It was recognized that a new disease, called nephrogenic systemic fibrosis (NSF), was associated with the use of the $Gd^{3+}$-based CAs. NSF was developed in patients with severe renal impairment, when the elimination of the CAs was slow. During the longer residence time of the Gd(III) complex in the body of patients a small amount of Gd(III) remained deposited, which presumably triggered the development of NSF [8-10]. More recently, the presence of Gd has been detected in different organs, including the brain of patients with normal renal function after a few repeated MR scans using CAs [11-14]. The presence of traces of non-chelated Gd(III) in the body of patients has raised concerns because of the potential toxicity of the Gd(III) ion. These problems with the use of the linear Gd(III)-based CAs turned the attention of researchers to the complexes of Mn(II) as potential contrast agents [15-16]. The relaxation effects of Mn(II) are known to be similar to those of Gd(III), but on the other hand, Mn(II) is an essential metal ion and some amount of the intravenously administered Mn(II) can be

eliminated relatively rapidly through the hepatobiliary system. Since the coordination number of Gd(III) is 8-9, while that of Mn(II) is often 6-7, the ligands used in the Gd(III)-based CAs can not be directly used for the complexation of Mn(II). Some examples are known, when the Mn(II) complexes with ligands performing well with Gd(III) are stable and inert, but the absence of inner sphere water molecule(s) results in negligible enhance in the contrast [17]. Another critical point is the lability/inertness of the complexes (the terms lability/inertness in this manuscript describe dissociation kinetics parameters of the complexes rather than the solvent exchange kinetics). The majority of the open-chain ligands form very labile complexes with Mn(II). The most shocking example is that of $[Mn(dtpa)]^{3-}$ which was found to dissociate within the dead-time of the stopped-flow instrument (ca. 8 msec) in the presence of Cu(II) as a ligand scavenger [18]. In order to find suitable ligands for Mn(II), a number of new linear and macrocyclic ligands were synthesized during the last years and the properties of their complexes were investigated extensively [15-24]. Amongst the hexadentate linear ligands edta forms the relatively stable $[Mn(edta)]^{2-}$ complex in which a water molecule occupies the seventh coordination site, but the kinetic inertness of the complex is also low, because of the flexible structure of the ligand [18]. The edta analogue *trans*-1,2-cdta (abbreviated as *t*-cdta through the text, Figure 1) is more rigid and it forms the more stable and more inert complex $[Mn(t\text{-}cdta)]^{2-}$ which seems to be suitable as a potential CA and recently was evaluated even in preclinical studies [25-26]. The behaviour of the cdta derivative ligands are likely similar to the parent ligand, so their Mn(II) complexes are promising for the preparation of Mn(II)-based MRI CAs [18, 22].

While the complexation properties of the *t*-cdta ligand have been studied extensively, there is very few knowledge about the complexes of the other stereoisomer, the *cis*-1,2-cdta ligand (abbreviated as *c*-cdta in the text). The donor atoms of *t*-cdta form a semi-rigid preorganized coordination cage, where metal ions of different size may enter and generally form complexes of high stability [27]. The maximum distance between the two *N*-donor atoms in *t*-cdta is 4 Å, while that in *c*-cdta is only 3.1 Å [28], so the coordination cage formed by the donor atoms of the *cis*- isomer is relatively small, anticipating a low stability of the complexes with *c*-cdta and large metal ions. Since the size of the Mn(II) ion is not too large and there are only very few data in the literature regarding the complexation of *c*-cdta, we decided to study its complexes with Mn(II) and with some other endogenous metal ions.
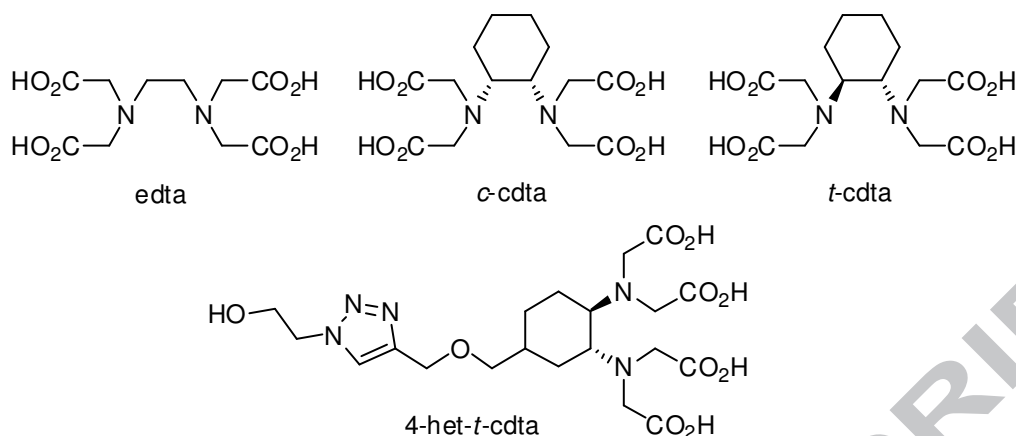
Figure 1. Formulae of the edta, *c*-cdta, *t*-cdta, 4-het-*t*-cdta ligands.

**Results and Discussion**

The synthesis of the *c*-cdta ligand (Scheme 1) was accomplished in a two-step reaction sequence starting from *cis*-cyclohexane-1,2-diamine, which was alkylated by using ethyl bromoacetate in the presence of Hünig's base (diisopropylethyl amine, dipea). The saponification of the tetraethyl ester with NaOH afforded the product which was purified by recrystallization from acidic (pH=2.0) aqueous solution.
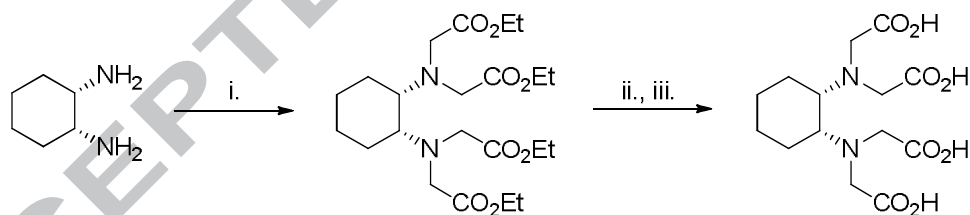


Scheme 1. The synthesis of the *c*-cdta chelator: i). 4.2 equivalent of ethyl bromoacetate, dipea, MeCN, 7 h reflux; ii). 6 equivalent of NaOH, EtOH, 24 h reflux; iii). cc HCl till pH = 2.0.

**Equilibrium studies**

In order to characterize the metal complexes as potential MRI contrast enhancement agents, one should consider their equilibrium and kinetic behaviour in biofluids, the proton relaxation effects, together with other parameters which determine the proton relaxation rates in the presence of these complexes. For the assessment of the equilibrium behaviour we have

5

determined the stability constant of the Mn(II) complex and those of the Mg(II), Ca(II), Zn(II) and Cu(II) complexes that may compete with the Mn(II) ion for the *c*-cdta ligand in biofluids. To obtain information about the kinetic inertness of [Mn(*c*-cdta)]$^{2-}$ complex, the rates of the exchange reactions occurring between the complex and the Cu(II) ion have been investigated, *vide infra*. These properties are already known for the [Mn(*t*-cdta)]$^{2-}$ complex, so the comparison of the behaviour of the two complexes is possible.

The protonation constants of the *c*-cdta ligand have been determined by pH-potentiometric titration. The protonation constants ($K_i^H$) defined by Equation (1), are presented in Table 1.

$$K_i^H = \frac{[H_iL]}{[H_{i-1}L][H^+]} \qquad \text{where i=1, 2, } \quad n \qquad \text{(eqn. 1)}$$

where i = 1, 2, …, 5, [H$_i$L], [H$_{i-1}$L] and [H$^+$] are the equilibrium concentrations of the H$_i$L and H$_{i-1}$L ligand species and the H$^+$ ions, respectively. The stability constants of the ML complexes ($K_{ML}$) are defined by Equation (2):

$$K_{ML} = \frac{[ML]}{[M][L]} \qquad \text{(eqn. 2)}$$

In Equation (2) [M], [ML] and [L] are the equilibrium concentrations of the M(II) metal ion, ML complex and L$^{4-}$ ligand, respectively (the charges of ions will be used only when it is necessary).

The metal ions and protons compete for the ligand, so at lower pH values protonated complexes can be formed. The protonation constants of complexes are defined as follows:

$$K_{MH_iL} = \frac{[MH_iL]}{[MH_{i-1}L][H^+]} \qquad \text{(eqn. 3)}$$

where i = 1 or 2, [M(H$_i$L)] and [M(H$_{i-1}$L)] are the concentration of the protonated complexes.

Table 1. Protonation constants of the *c*-cdta, *t*-cdta and edta ligands and stability constants of their Mg(II), Ca(II), Zn(II), Cu(II) and Mn(II) complexes (log *K* values, 25°C, 0.15 NaCl).

|  |  | $c$-cdta[a] | $c$-cdta[b] | $t$-cdta[c] | $t$-cdta[b] | edta[c] |
|---|---|---|---|---|---|---|
| **H⁺** | $\log K_1^H$ | **11.00(1)** | 10.70 | 9.54 | 11.70 | 9.28 |
|  | $\log K_2^H$ | **5.20(1)** | 5.21 | 5.97 | 6.12 | 6.04 |
|  | $\log K_3^H$ | **3.41(1)** | 3.50 | 3.60 | 3.52 | 2.72 |
|  | $\log K_4^H$ | **2.30(1)** | 2.44 | 2.52 | 2.43 | 1.99 |
|  | $\log K_5^H$ | **1.41(1)** | – | 1.46 | – | 1.11 |
|  | $\sum \log K_i^H$ | **23.32** | 21.85 | 23.09 | 23.77 | 21.14 |
| **Mg²⁺** | $\log K_{ML}$ | **9.01(2)** | 8.38 | 9.14 | 11.07 | 7.61 |
|  | $\log K_{MHL}$ | **4.72(6)** | 4.44 | 3.53 | – | – |
| **Ca²⁺** | $\log K_{ML}$ | **9.65(2)** | 9.45 | 10.23 | 13.15 | 9.53 |
|  | $\log K_{MHL}$ | **4.55(5)** | 4.11 | 3.53 | – | 2.92 |
| **Mn²⁺** | $\log K_{MnL}$ | **14.19(2)** | – | 14.32[d] | 17.48 | 12.46[d] |
|  | $\log K_{MnHL}$ | **2.85(3)** | – | 2.90[d] | 2.8 | 2.95[d] |
|  | $\log K_{MnH2L}$ | – | – | 1.89[d] | – | –[d] |
|  | pMn[e] | **7.82** | – | 8.68 | – | 7.83 |
| **Zn²⁺** | $\log K_{ML}$ | **17.06(1)** | – | 16.75 | 19.37 | 15.92 |
|  | $\log K_{MHL}$ | **2.76(1)** | – | 2.57 | 2.9 | 3.23 |
|  | $\log K_{MH2L}$ | – | – | – | – | 1.50 |
| **Cu²⁺** | $\log K_{ML}$ | **18.3(1)**[f] | – | 19.78[f] | 22.0 | 19.02[f] |
|  | $\log K_{MHL}$ | **3.65(3)** | – | 2.91 | 3.1 | 3.15 |
|  | $\log K_{MH2L}$ | – | – | 1.10 | – | 2.04 |

[a] this work; [b] Ref. [27]; [c] 0.15 M NaCl, 25°C from the diploma work of Veronika Józsa, 2015, University of Debrecen, Debrecen, Hungary; [d] Ref. [18]; [e] calculated by using $c_{Mn}=c_{Lig}=0.01$ mM at pH=7.4 according Tóth et al. [29]; [d] determined by simultaneous fitting of the UV-vis and pH-potentiometic data.

The protonation constants of $c$-cdta determined in this work at 25°C in 0.15 M NaCl solution (Table 1) agree relatively well with those reported in the literature [27] (20°C and 0.1 M KCl), indicating that the interaction of $c$-cdta with the Na⁺ and K⁺ ions is negligible. The $t$-cdta ligand behaves differently, since its $\log K_1^H$ value in 0.15 M KNO₃ is much higher (11.70) than in 0.15 M NaCl (9.54), because the stability constant of the $[Na(t\text{-cdta})]^{2-}$ complex is relatively high ($\log K_{NaL} = 4.4$) [27], while the interaction of the ligand with K⁺ is very week. The different behaviour of the two ligands indicates that the coordination cage

7

formed by the two iminodiacetate (ida) groups of *c*-cdta is too small to accommodate the larger M(I) metal ions, while in the case of *t*-cdta the coordination cage is larger, where even a Na$^+$ ion can enter.

The stability constant of the Mg(II)- and [Ca(*c*-cdta)]$^{2-}$ complexes obtained in this work are comparable with those published in the literature (Table 1). For the *c*-cdta complexes of Mn(II), Zn(II) and Cu(II) there are not any stability constant data in literature. The stability constants of complexes formed with the *c*-cdta, *t*-cdta and edta ligands in 0.15 M NaCl (Table 1) do not differ considerably, because of the formation of the [Na(*t*-cdta)]$^{3-}$ complex. Considering the formation of Na$^+$ complexes, it is more correct to compare the log $K_{ML}$ values of *c*-cdta complexes with those log $K_{ML}$ values obtained for the *t*-cdta complexes at 0.1 M KCl ionic strength. This comparison shows that the stability constants of the [M(*c*-cdta)]$^{2-}$ complexes are lower by 2-3 log units than those of the [M(*t*-cdta)]$^{2-}$ complexes (Table 1).

The paramagnetic metal ions used as a component of the MRI CAs result in high proton relaxation rates. Since the free metal ions are toxic, their complexes are used as CAs. The longitudinal relaxation rate of water protons ($1/T_1$ where $T_1$ is the longitudinal relaxation time) in the presence of Mn(II) ions is significantly higher than in the presence of [Mn(*c*-cdta)]$^{2-}$ or [Mn(*t*-cdta)]$^{2-}$. The relaxation effect of paramagnetic ions and complexes are expressed by their relaxivity values. The relaxivity ($r_{1p}$, mM$^{-1}$s$^{-1}$) is the enhancement of the longitudinal water proton relaxation rate referred to 1.0 mM concentration of the paramagnetic species. The relaxivity of the [Mn(H$_2$O)$_6$]$^{2+}$ ion at 25°C and 20 MHz is 7.94 mM$^{-1}$s$^{-1}$, while that of the [Mn(*c*-cdta)]$^{2-}$ complex is 3.79 mM$^{-1}$s$^{-1}$. This latter $r_1$ value is similar to that of the [Mn(edta)]$^{2-}$ (3.23 mM$^{-1}$s$^{-1}$) and [Mn(*t*-cdta)]$^{2-}$ (3.62 mM$^{-1}$s$^{-1}$) complexes, in which one water molecule is coordinated in the inner sphere of Mn(II).

The formation of [Mn(*c*-cdta)]$^{2-}$ complexes could be followed by measuring the water proton relaxation rates in equilibrium solutions of 1.0 mM Mn(II) and 1.0 mM *c*-cdta as a function of pH. At pH<2 only [Mn(H$_2$O)$_6$]$^{2+}$ is present, resulting in high $1/T_1$ values (Fig. 2). With the increase of pH, MnHL and MnL complexes are formed, so that the proton relaxation rates decrease because the water molecules are displaced from the inner sphere of Mn$^{2+}$. Once the formation of [Mn(L)] complex is complete (at about pH>5,) the $1/T_1$ values are constant (this constant $1/T_1$ value is the relaxivity of the MnL complex). In Figure 2 the species distribution curves (calculated from the equilibrium data for the 1.0 mM Mn(II) - 1.0 mM *c*-cdta system) are also presented (together with the $1/T_1$ values). The data in Figure 2 indicate

8

that the decrease of the proton relaxation rates with the increase of pH occurs parallel with the formation of the MnHL and MnL complexes. The good agreement in the trend of the data obtained by pH-potentiometry and relaxometry indicates the reliability of the equilibrium data.
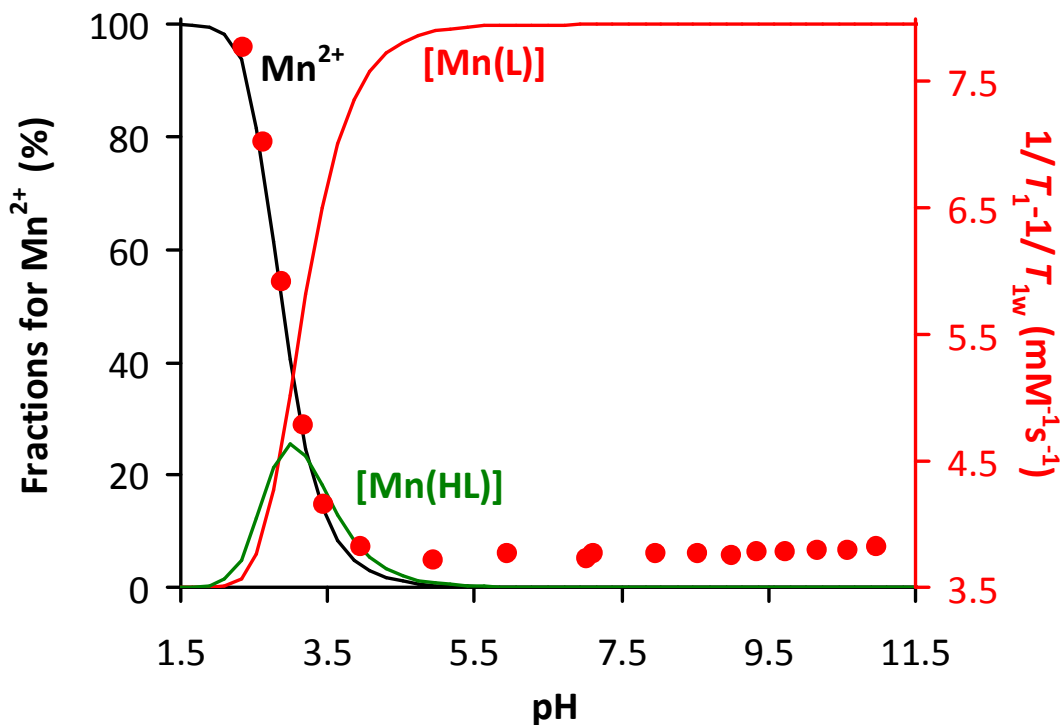


Figure 2. Species distribution curves and the relaxation rate $(1/T_1-1/T_{1w})$ profile (red points) of 1.021 mM $[Mn(c\text{-cdta})]^{2-}$ as a function of pH (T = 25 $^{o}$C, I=0.15 M NaCl, 20 MHz).

As it was underlined several times in the literature, reliable stability data for Cu(II) – APC complexes can be obtained either by competition method with the use of auxiliary ligand (the equilibrium of the Cu(II) – auxiliary ligand system must be well known), or it can be accessed by using multiple methods simultaneously (e.g. UV-vis spectrophotometry applicable also in very acidic conditions and pH-potentiometry) [31]. The absorption spectra of the $[Cu(c\text{-cdta})]^{2-}$ complex as a function of $H^+$ ion concentration is shown on Figure 3. The spectrophotometric data were fitted simultaneously with the pH-potentimetric titration data and the stability constants determined are shown in Table 1. In line with the equilibrium data obtained for other metal ions studied, the stability constant of the $[Cu(c\text{-cdta})]^{2-}$ complex is

9

lower than the value of the corresponding $[Cu(t\text{-cdta})]^{2-}$ complex determined under identical conditions (the difference is ca. 0.7 log units).
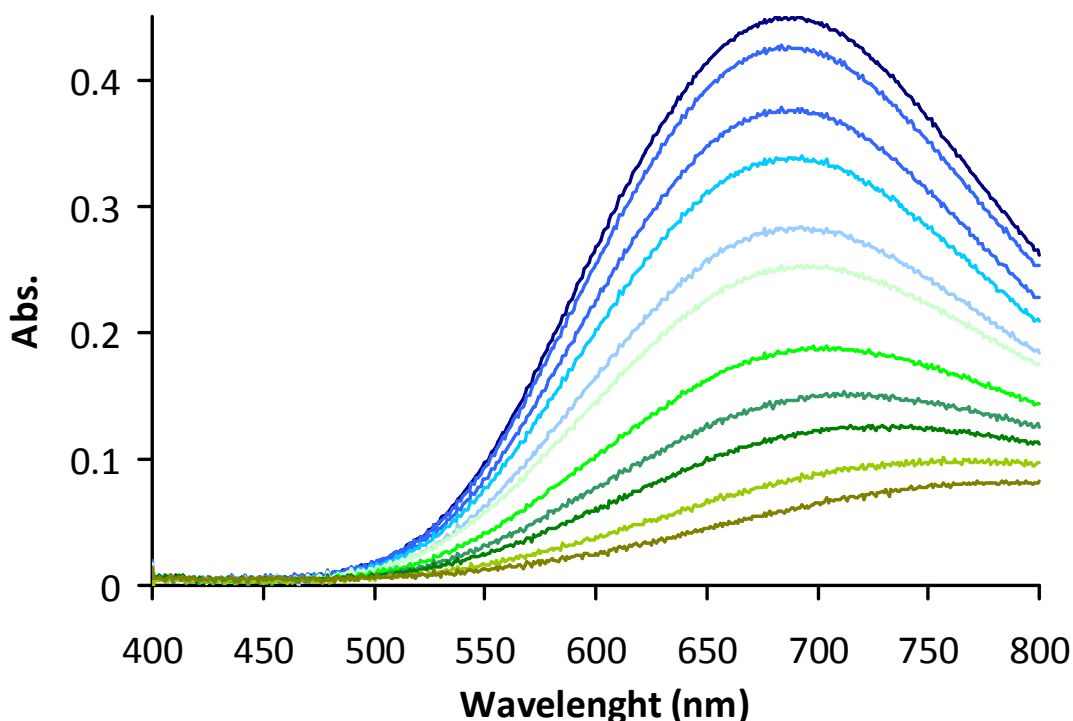


Figure 3. Absorption spectra of the $[Cu(c\text{-cdta})]^{2-}$ system as a function of $[H^+]$. Conditions: $[c\text{-cdta}^{4-}] = 3.528$ mM, $[Cu(II)] = 3.410$ mM, 25 $^o$C, 1.0 M $(Na^++H^+)Cl^-$, $c_{H+}$ in the samples are as follows: 12.1; 18.8; 33.9; 49.0; 75.9; 101.0; 156.8; 205.0; 253.3; 349.8 and 462.4 mM (from top to bottom).

## Dissociation kinetics of $[Mn(c\text{-cdta})]^{2-}$ complex

The fate of the MRI CAs in biological fluids is strongly influenced by their kinetic inertness, that is an important property in determining the extent of dissociation of the complex while present in the body. For the Gd(III)-based CAs it was generally assumed that the deposition of Gd in the body was the result of the dissociation of Gd(III) complexes, that occurred through transmetallation reactions with endogenous metal ions like Zn(II), Cu(II) and Ca(II) [33, 34]. To obtain information about the kinetic properties of CAs, the rates of the metal-exchange reactions are generally studied between the Gd(III) or Mn(II) complex and an exchanging metal ion, very often Cu(II), because in this case the reaction can easily be

10

followed by spectrophotometry. The kinetic behaviour of $[Mn(c\text{-cdta})]^{2-}$ was studied similarly by following the exchange reactions depicted in Equation (4):

$$[Mn(c\text{-cdta})]^{2-} + Cu(II) \rightleftharpoons [Cu(c\text{-cdta})]^{2-} + Mn(II) \qquad \text{(eqn. 4)}$$
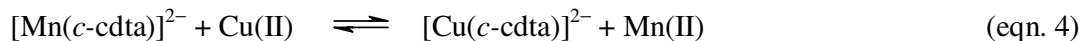
Since the stability constant of $[Cu(c\text{-cdta})]^{2-}$ is much higher than that of $[Mn(c\text{-cdta})]^{2-}$ (Table 1), reaction (4) takes place to completeness in the presence of Cu(II) excess (10-40 fold of Cu(II) excess was used). Under such conditions the reactions can be treated as pseudo-first-order processes kinetically. The rate of the exchange reaction (4) is directly proportional to the concentration of the complex and can be expressed as follows:

$$-\frac{d[Mn(L)]_t}{dt} = k_{obs}[Mn(L)]_t \qquad \text{(eqn. 5)}$$

In Equation (5) $k_{obs}$ is a pseudo-first-order rate constant, $[Mn(L)]_t$ is the total concentration of complexes containing the $[Mn(c\text{-cdta})]^{2-}$ species. The rates of the exchange reactions (4) have been studied at four different Cu(II) concentrations in the pH range 4.03 – 5.03. The $k_{obs}$ values obtained are shown in Figure 4.
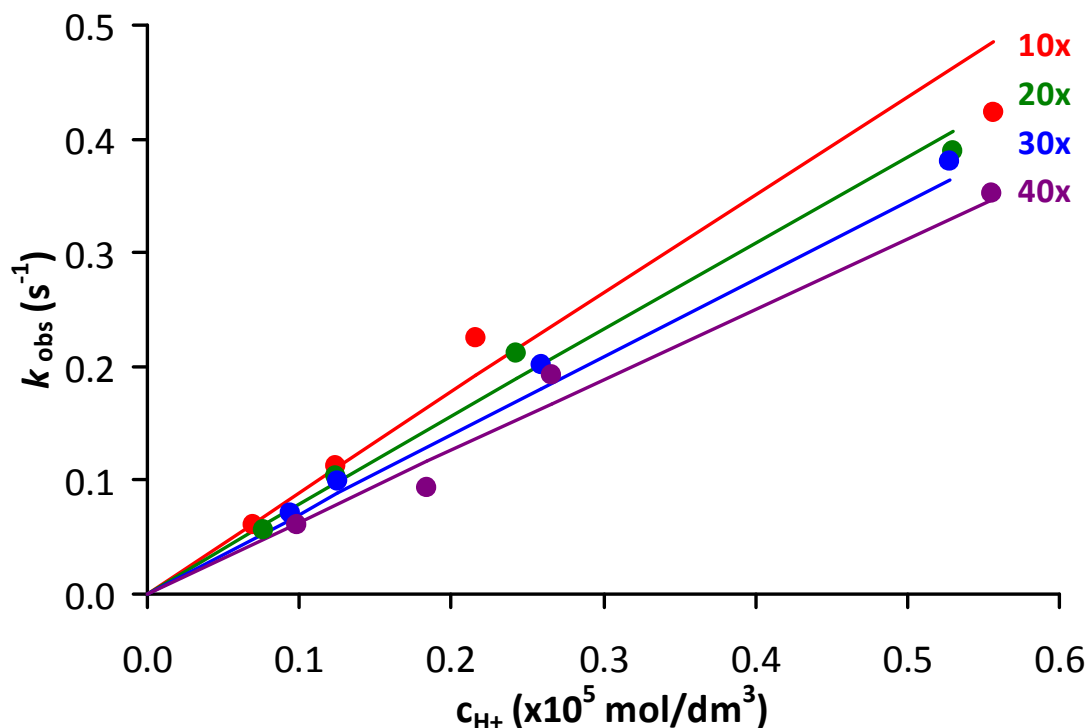


11

Figure 4. The rate constants ($k_{obs}$) characterizing the exchange reactions of [Mn($c$-cdta)]$^{2-}$ (0.4 mM) with Cu(II) measured by stopped-flow method. The Cu(II) concentrations are 4.0 mM (red), 8.0 mM (green), 12.0 mM (blue) and 16.0 mM (wine-red) (25°C, 0.15 M NaCl).

The kinetic data shown in Figure 4 reveal that the $k_{obs}$ values are directly proportional to [H$^+$], the exchange reactions showing first-order dependence on the H$^+$ ion concentration. The dependence of the $k_{obs}$ values on the Cu(II) concentration is surprising, because the increase in the Cu(II) concentration results in a slight decrease in the reaction rates, so that Cu(II) ions depress the rate of the exchange reactions. Similar phenomena were observed previously for the reaction of [Mn($t$-cdta)]$^{2-}$ with Cu(II) and for the reactions between [Cd($t$-cdta)]$^{2-}$ and Pb(II) or Cu(II) ions [18, 35]. The effect of the Cu(II) ions on the reaction rates can be interpreted by the formation of dinuclear [Mn($c$-$cdta$)Cu] complexes, where presumably one acetate group of [Mn($c$-cdta)]$^{2-}$ is coordinated to the Cu(II) ion and so the probability of protonation decreases (in fact [Mn($c$-cdta)Cu] is a "dead-end" complex). Since the reaction rate does not increase with the increase of the Cu(II) concentration, the exchange reactions do not take place with the direct attack of the Cu(II) ion. On the basis of the experimental data we came to the conclusion that the exchange reactions between the [Mn($c$-cdta)]$^{2-}$ and Cu(II) ion occur through the dissociation mechanism. After the rate determining dissociation of the complex, the released $c$-cdta ligand rapidly reacts with the Cu(II) ions with the formation of [Cu($c$-cdta)]$^{2-}$. The dissociation of the [Mn($c$-cdta)]$^{2-}$ complex can take place spontaneously and by the assistance of H$^+$ ions. The spontaneous dissociation is presumably very slow, while the proton assisted dissociation occurs relatively rapidly at pH values around 4-5. The protonation of [Mn($c$-cdta)]$^{2-}$ presumable occurs at a carboxylate group (log $K_{MHL}$ = 2.85), but for the dissociation of the complex the proton must be transferred to a N atom, when the protonated iminodiacetate (ida) group is not coordinated anymore and this intermediate may dissociate (or the complex may be re-formed by the dissociation of the proton). Considering the possible reaction pathways, the rate of dissociation of the complex can be expressed by Equation (6)

$$-\frac{[Mn(L)]_t}{dt} = k_0[Mn(L)] + k_{MnHL}[Mn(HL)] \qquad \text{(eqn. 6)}$$

12

where $k_0$ and $k_{MnHL}$ are the rate constants characterizing the dissociation of the MnL and MnHL complexes, respectively.

Comparing the total concentration of the complex $[Mn(c\text{-cdta})]^{2-}$ ($[Mn(L)]_t = [Mn(L)] + [Mn(HL)] + [Mn(L)Cu]$), Equation (5) and (6), for the $k_{obs}$ value Equation (7) is obtained:

$$k_{obs} = \frac{k_0 + k_{MnHL} \cdot K_{MnHL} \cdot [H^+]}{1 + K_{MnHL}[H^+] + K_{MnLCu}[Cu^{2+}]} \qquad \text{(eqn. 7)}$$

The term $K_{MnHL}[H^+]$ in the denominator of Equation (7) is very small in the pH range 4.03 – 5.03, so it can be neglected. For the calculation of the unknown parameters Equation (7) has been used as follows:

$$k_{obs} = \frac{k_0 + k_1 \cdot [H^+]}{1 + K_{MnLCu}[Cu^{2+}]} \qquad \text{(eqn. 8)}$$

where $k_1 = k_{MnHL} K_{MnHL}$.

By fitting the $k_{obs}$ values presented in Figure 4 to Equation (8) the $k_0$, $k_1$ and $K_{MnLCu}$ values have been calculated and presented in Table 2. The $k_0$ value is very low, so it can be neglected.

Table 2. Rate and equilibrium constants characterizing the dissociation rates of the $[Mn(c\text{-cdta})]^{2-}$, $[Mn(t\text{-cdta})]^{2-}$ and $[Mn(edta)]^{2-}$ complexes.

| | *c*-cdta | *t*-cdta[a,b] | edta[a,b] |
|---|---|---|---|
| $k_1$ ($M^{-1}s^{-1}$) | $(1.02\pm0.09)\times10^5$ | $4.0\times10^2$ | $5.2\times10^4$ |
| $k_2$ ($M^{-2}s^{-1}$) | – | – | $2.3\times10^8$ |
| $k_3$ ($M^{-1}s^{-1}$) | – | – | $45\pm8$ |
| $K_{MnLCu}$ | $79\pm23$ | 79 | – |

13

| log $K_H$ | 2.85[c] | 2.90[c] | 2.65[c] |
|---|---|---|---|
| $t_{1/2}$[d] (h) | 0.47 | 12 | 0.076 |

[a] Ref [18]; [b] for [Mn($t$-cdta)]$^{2-}$ $k_1 = 3.2 \times 10^2$ M$^{-1}$s$^{-1}$ and $t_{1/2} = 15$ h while for [Mn(edta)]$^{2-}$ $k_3 = 3.0 \times 10^{-1}$ M$^{-1}$s$^{-1}$, $k_4 = \sim 4.8 \times 10^1$ M$^{-2}$s$^{-1}$ and log $K_{MnHL} = 3.10$ were found in Ref. [36]; [c] determined by pH-potentiometry and fixed in the data fitting; [d] calculated at pH = 7.4 in the presence of $c_{Cu2+} = 1 \times 10^{-5}$ M.

In Table 2, the $k_1$ rate constants and $K_{MnLCu}$ stability constants obtained for the [Mn($c$-cdta)]$^{2-}$ complex are compared with those of the [Mn($t$-cdta)]$^{2-}$. The presented data indicate that the $k_1$ dissociation rate constant of [Mn($c$-cdta)]$^{2-}$ is approximately 250 times higher than that of [Mn($t$-cdta)]$^{2-}$. This difference is shown in the values of the half-life of dissociation, that is much longer for complex [Mn($t$-cdta)]$^{2-}$. The results of these studies indicate that the kinetic inertness of the Mn(II) complex formed with the $c$-cdta isomer is significantly lower than that of the $t$-cdta isomer.

## $^{17}$O and NMRD measurements

The nuclear magnetic relaxation dispersion (NMRD) profile of the [Mn($c$-cdta)]$^{2-}$ was measured at three different temperatures (298, 310 and 323 K) in the frequency range 0.01-80 MHz to gain information on the relaxation properties of the complex (Figure 5). The NMRD profiles show a single dispersion at 1-10 MHz which is typical of low molecular weight Mn$^{2+}$ complexes. Their temperature dependence indicates that the relaxivity of the complex is limited by fast rotation. Several physicochemical parameters affect the relaxivity of a paramagnetic metal complex, such as the water exchange rate, the electron spin relaxation parameters and the rotational correlation time. The temperature dependence of the transverse and longitudinal $^{17}$O relaxation rates can provide information on the water exchange rate ($k_{ex}$) and the rotational correlation time ($\tau_R$), respectively, while the chemical shift is related to the number of the water molecules directly coordinated to the paramagnetic metal center ($q$). Variable temperature transverse and longitudinal relaxation rates and chemical shifts were measured for an aqueous solution of [Mn($c$-cdta)]$^{2-}$ and for a diamagnetic reference at 9.4 T. The $T_1$ values showed negligible difference between the Mn(II) complex and the reference, thus were not included in the analysis. The reduced $^{17}$O transverse relaxation rates, 1/$T_{2r}$, and chemical shifts, $\Delta \omega_r$, have been fitted according to the Swift-Connick equations, by assuming

a simple exponential behaviour for the electron spin relaxation. The water exchange rate, $k_{ex}^{298}$, its activation enthalpy, $\Delta H^{\neq}$, and $1/T_{1e}^{298}$ were calculated (the activation energy of electron spin relaxation was fixed to 1 kJ/mol). The hydration number was fixed to $q=1$ based on analogy to $[\text{Mn}(t\text{-cdta})]^{2-}$ and on the relaxivity value measured at 20 MHz ($r_{1p}=3.79$ mM$^{-1}$s$^{-1}$, $r_{1,[\text{Mn}(t\text{-cdta})]2-}=3.62$ [18]) We have attempted to determine the hydration number of the complex by using Gale's method based on the maximum value of the transverse $^{17}$O relaxation rate however the q obtained (q = 0.50±0.20) seems to be an underestimation since the relaxivity of the given complex as well as the results of DFT calculations (vide supra) are being consistent with q=1.[37] To characterize the rotational dynamics of the complex, the $^1$H NMRD data were analyzed by the Solomon-Bloembergen-Morgan (SMB) [38] and Freed models [39] (inner- (IS) and outer-sphere (OS) relaxation mechanisms) and the Swift-Connick [40, 41] equations related to solvent exchange (see Supporting Information). The parameters for water exchange were fixed to those determined from the $^{17}$O NMR study. The distances between the metal ion and the inner and outer sphere water protons were also fixed ($r_{\text{MnH}} = 2.83$ Å and $a_{\text{MnH}} = 3.6$ Å), as well as the diffusion coefficient and its activation energy ($D_{\text{MnH}} = 26 \times 10^{-10}$ m$^2$s$^{-1}$ and $E_{\text{MnH}} = 18$ kJ/mol$^{-1}$ [29]) and the activation energy of the modulation of the zero-field-splitting ($E_v = 1.0$ kJ/mol). The values of the electron relaxation parameters $\tau_v^{298}$ and $\Delta^2$ were found to be 21±2 ps and $(1.0\pm0.1)\times10^{20}$ s$^{-2}$, respectively. The best-fit parameters obtained are given in Table 3 and compared with those of $[\text{Mn}(t\text{-cdta})]^{2-}$ and $[\text{Mn}(4\text{-het-cdta})]^{2-}$ complexes [42, 43]. The experimental data and the fitted curves are shown in Figures 5 and 6.
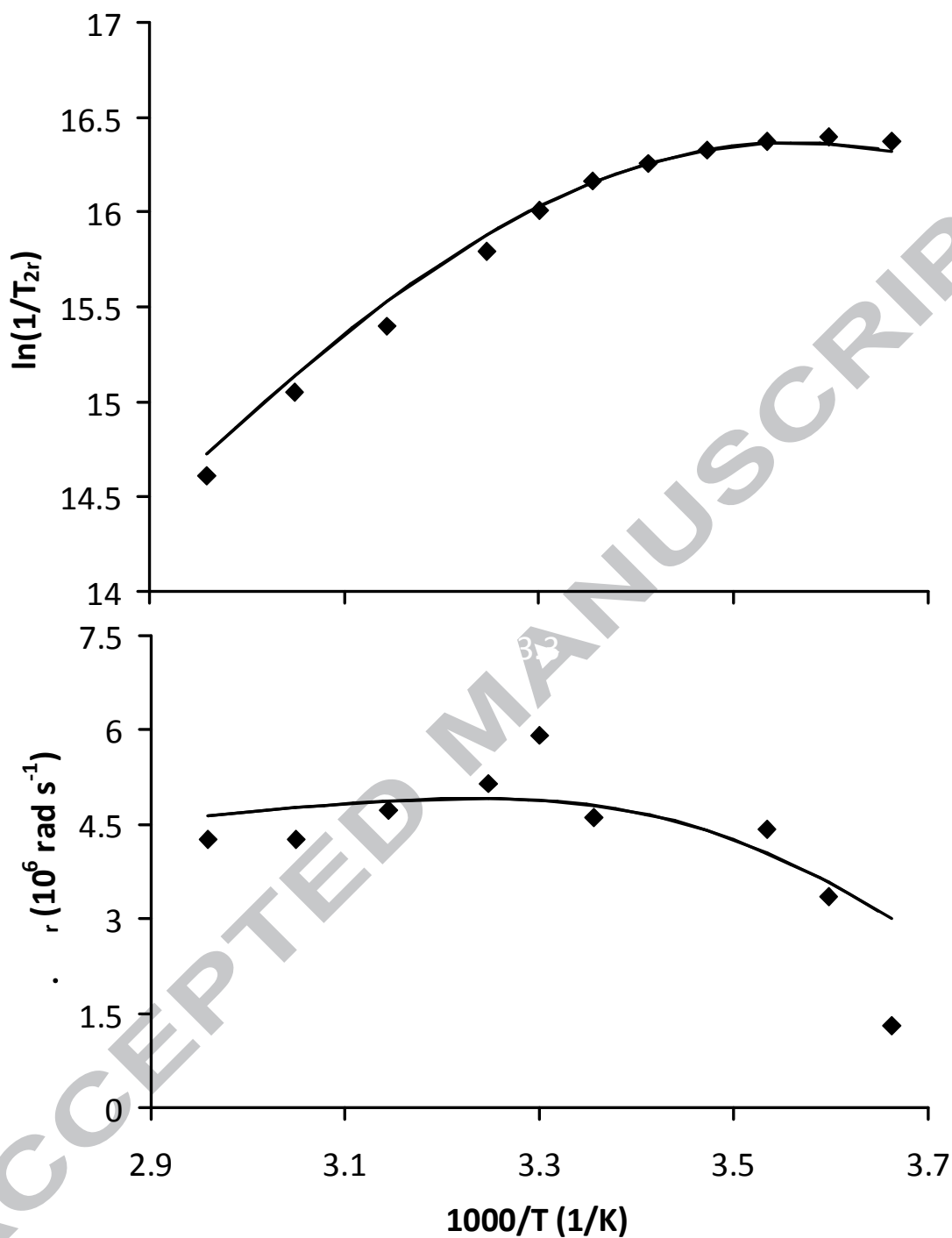
15

Figure 5. Variable temperature reduced transverse $^{17}O$ relaxation rates (top) and chemical shifts (bottom) recorded for $[Mn(c\text{-cdta})]^{2-}$ (B = 9.4 T). The solid lines correspond to the fit of the data.

Table 3. Parameters obtained from the analysis of $^{17}O$ NMR and $^{1}H$ NMRD data for the $[Mn(c\text{-cdta})(H_2O)]^{2-}$ complex.

| Parameter | [Mn(c-cdta)]²⁻ | [Mn(t-cdta)]²⁻ [c] | [Mn(4-het-cdta)]²⁻ [d] |
|---|---|---|---|
| $k_{ex}^{298}$ (x10⁷ s⁻¹) [a] | 22.5 ± 0.5 | 14.0 | 17.6 |
| $\Delta H^{\ddagger}$ (kJ mol⁻¹) [a] | 42.0 ± 0.8 | 42.5 | 36.2 |
| $\Delta S^{\ddagger}$ (J K⁻¹ mol⁻¹) [a] | +56 ± 4 | – | – |
| $A_O/\hbar$ (10⁶ rad s⁻¹) [a] | -42.7 ± 0.9 | -26.4 | -40 |
| $1/T_{1e}^{298}$ (x10⁷/ s⁻¹) [a] | 27.0 ± 0.5 | 0.65 | 7 |
| $E_{rH}$ (kJ mol⁻¹) [b] | 20.4 ± 0.7 | – | 26.2 |
| $\tau_{rH}^{298}$ (ps) [b] | 74 ± 2 | – | 104.9 |

[a] from ¹⁷O NMR; [b] from NMRD; [c] Ref. [42]; [d] Ref. [44].


As Figure 5 shows, the reduced transverse ¹⁷O relaxation rates undergo a changeover at ~290 K between the fast and intermediate water exchange regime. Importantly, the water exchange rate has a significant contribution to the overall correlation time ($1/\tau_c = k_{ex} + 1/T_{1e}$; $k_{ex}$ varying from 10 to 80% in the temperature range 273-338 K), which makes possible to accurately determine $k_{ex}$. The $k_{ex}^{298}$ value characterizing the water exchange of [Mn(c-cdta)]²⁻ is ca. 60% higher than that of [Mn(t-cdta)]²⁻. The high positive activation entropy points to a dissociative mechanism, as would be expected for a seven-coordinated Mn(II) complex.

On the other hand, $k_{ex}^{298}$ is half of the value determined for [Mn(edta)]²⁻ (47.1×10⁷ s⁻¹) [45]. This is related to the more rigid structure of the cdta⁴⁻ ligands which detains the rearrangement of the coordination environment during the water exchange process. The water exchange is also several times slower on [Mn(c-cdta)]²⁻ than on the 1,4-do2a or do1a complexes, having a very different, macrocyclic structure [46]. The rotational correlation time ($\tau_{rH}^{298}$) obtained from the analysis of the relaxivity data is in the usual order of magnitude of typical low molecular weight complexes.
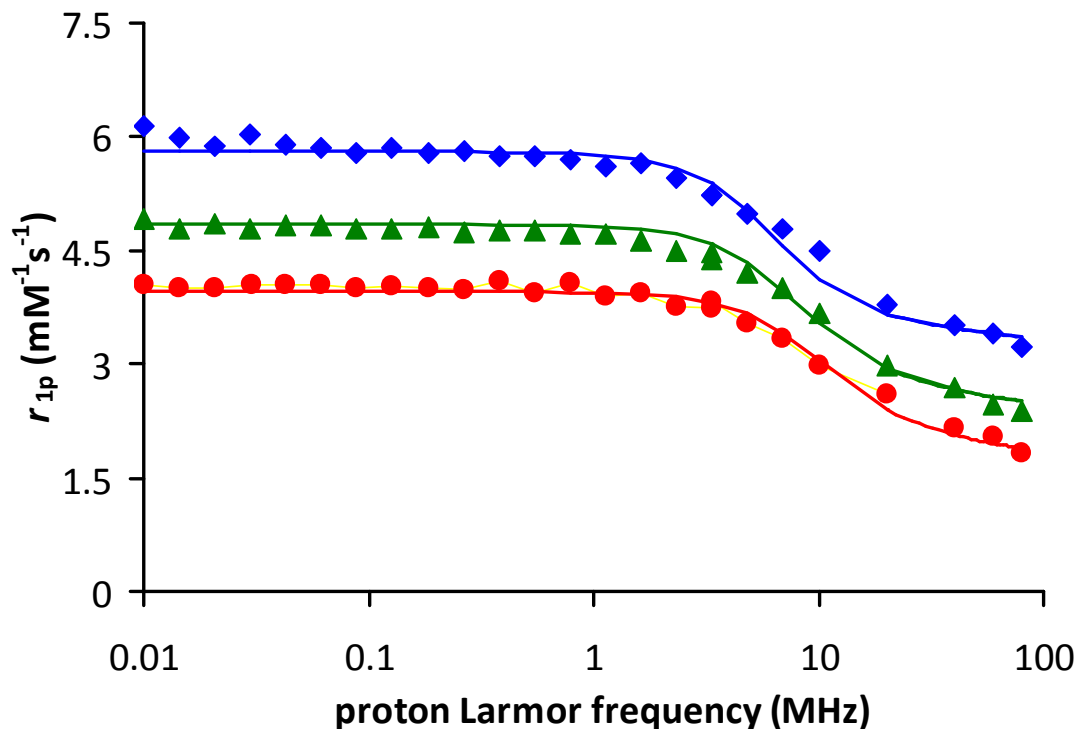
Figure 6. ^{1}H NMRD profiles of [Mn(*c*-cdta)]$^{2-}$ at 25 °C (♦), 37 °C (▲) and 50 °C (●).

**DFT study**

Aiming shed light on the reasons behind the different behaviour of the [Mn(*c*-cdta)(H$_2$O)]$^{2-}$ and [Mn(*t*-cdta)(H$_2$O)]$^{2-}$ complexes, we carried out a theoretical DFT study. These calculations were performed with the explicit inclusion of two second-sphere water molecules, which were previously found to be necessary for an accurate determination of Mn-O$_{water}$ bond distances and [17]O hyperfine coupling constants $A_O/\hbar$ [47]. The X-ray structure of the ammonium salt of [Mn(*t*-cdta)(H$_2$O)]$^{2-}$ was reported [48]. Our DFT calculations (M062X/TZVP, see details below) provide bond distances of the metal coordination environment in excellent agreement with the solid state data (Supporting Information). The structure obtained using DFT for [Mn(*c*-cdta)(H$_2$O)]$^{2-}$ is very similar to that of the *trans* analogue, with the bond distances in the two complexes differing by > 0.035 Å (Figure 7). An overlay of the two calculated structures corroborates the very similar coordination environments of the two structures (Supporting Information). In spite of the minor differences in the metal coordination environments, DFT calculations indicate that the [Mn(*t*-cdta)(H$_2$O)]$^{2-}$ complex is considerably more stable than the *cis* analogue. The free energy

18

difference between the two complexes favors the *trans* isomer by 35.4 kJ mol$^{-1}$, which is compatible with a higher stability of [Mn(*t*-cdta)(H$_2$O)]$^{2-}$ by several orders of magnitude. This is likely the consequence of the more strained geometry of the ligand in [Mn(*c*-cdta)(H$_2$O)]$^{2-}$ to accommodate the relatively large Mn$^{2+}$ ion.
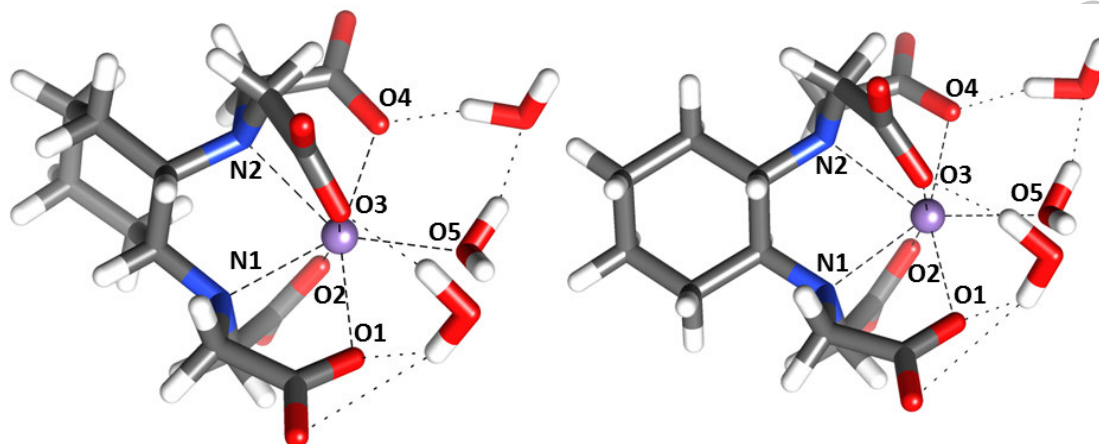


Figure 7. Structures of the [Mn(*c*-cdta)(H$_2$O)]$^{2-}$·2H$_2$O (left) and [Mn(*t*-cdta)(H$_2$O)]$^{2-}$·2H$_2$O (right) systems obtained with DFT calculations.

The bond distances involving the metal ion and the coordinated water molecule (Mn-O5) obtained for the two systems are very similar (2.264 and 2.271 Å for the *cis* and *trans* complexes, respectively). Since the water exchange reaction in these complexes is expected to follow a dissociative mechanism, one would expect similar activation enthalpies for the two systems, as the rupture of the Mn-O5 bond to reach the six-coordinated transition state should require similar energies. Thus, we explored the potential energy surface of the [Mn(*c*-cdta)(H$_2$O)]$^{2-}$·2H$_2$O and [Mn(*t*-cdta)(H$_2$O)]$^{2-}$·2H$_2$O systems by increasing the Mn-O5 distances, which eventually led to the six coordinated systems [Mn(*c*-cdta)]$^{2-}$·3H$_2$O and [Mn(*t*-cdta)]$^{2-}$·3H$_2$O. The enthalpy difference of the seven- and six-coordinated forms favours the *q* = 1 structures by very similar values (24.0 and 23.4 kJ mol$^{-1}$ for the *c*-cdta and *t*-cdta complexes, respectively), as would be expected considering the similar Mn-O5 bond distances. However, the corresponding relative free energies differ significantly (15.1 and 16.8 kJ mol$^{-1}$ for the *c*-cdta and *t*-cdta complexes, respectively), and suggest a higher free energy barrier for the water exchange in [Mn(*t*-cdta)(H$_2$O)]$^{2-}$, which agrees with the experimental evidence. Thus, the faster water exchange rate of [Mn(*c*-cdta)(H$_2$O)]$^{2-}$ obtained

19

from ^{17}O NMR measurements appears to be related to entropy factors rather than to important differences in the environments around the coordinated water molecules.

DFT calculations give values of the hyperfine coupling constants $A_O/\hbar$ of $-44.9\times10^6$ and $-44.6\times10^6$ rad s$^{-1}$ for the [Mn(*c*-cdta)(H$_2$O)]$^{2-}$ and [Mn(*t*-cdta)(H$_2$O)]$^{2-}$ complexes, respectively. The first value is in excellent agreement with the one obtained from ^{17}O NMR measurements in this study ($A_O/\hbar = -42.7\times10^6$ rad s$^{-1}$), while the second is somewhat higher than the experimental value reported for [Mn(*t*-cdta)]$^{2-}$ using only $T_2$ relaxation data ($-26.4\times10^6$ rad s$^{-1}$) [42]. The close agreement between the experimental and calculated hyperfine coupling constant of [Mn(*c*-cdta)(H$_2$O)]$^{2-}$ confirms that the assumption of $q = 1$ is correct.

## Summary

Our efforts to find suitable ligand for Mn(II) complexation started from equilibrium, kinetic and relaxometric characterization of Mn(II) complexes formed with commercially available open-chain ligands a few years ago [18]. The studies performed revealed that the rigid *t*-cdta forms relatively inert complex with Mn(II) ion (the half-life of the dissociation is expected to be 12 hours near to physiological conditions). However, to best of our knowledge Mn(II) complexes of other rigid edta derivative ligands such as *cis*-1,2-cyclohexanediamine or *o*-phenylenediamine tetraacetates (e.g. *c*-cdta or phdta) were not studied in detail in this respect. The combined experimental and DFT study presented in this work show that the [Mn(*c*-cdta)(H$_2$O)]$^{2-}$ and [Mn(*t*-cdta)(H$_2$O)]$^{2-}$ complexes present very similar solution structures in terms of the geometry around the metal coordination environment. However, the better pre-organization of the *trans* derivative for the coordination of relatively large metal ions such as Mn$^{2+}$ results in rather different properties.

The thermodynamic, kinetic (solvent and dissociation kinetic data) and relaxation parameters expressed in terms of water exchanges rates and relaxivity values (at 25 °C) are collected in the following table. The data collected for these hexadentate chelators indeed indicate that the Mn(II) complexes of these ligands differ notably. The most pronounced difference is seen for the dissociation kinetic data as the Mn(II) complex formed by the *cis*-derivative ligand shows properties similar to those seen for other labile complexes of linear edta-type ligands [18] whereas the *t*-cdta forms relatively inert Mn(II) complex. Moreover, the stability (especially the conditional stability) behaves alike by making the *trans*-1,2-

cyclohexanediamine unit to be an excellent "building block" when tailoring inert Mn(II) complexes for safe MRI applications.

Table 4. Comparison of the most important physico-chemical data of the Mn(II) complexes formed with *t*-cdta and *c*-cdta ligands.

| Parameter | $[Mn(c\text{-cdta})]^{2-}$ | $[Mn(t\text{-cdta})]^{2-}$ [a] |
|---|---|---|
| $\log K_{[Mn(L)]}$ | 14.19 | 14.32 |
| pMn[b] | 7.82 | 8.68 |
| $t_{1/2}$ (h)[c] | 0.47 | 12 |
| $k_{ex}^{298}$ (x$10^7$ s$^{-1}$) | 22.5 | 14.0[d] |
| $r_{1p}^{298}$ [e] | 3.79 | 3.62 |

[a] Ref. [18]; [b] pMn values were calculated at pH=7.4 by using 0.01 mM Mn(II) and ligand concentration as suggested by É. Tóth and co-workers [29]; [c] the half-lives (h) of dissociation were extrapolated to pH=7.4 by using 0.01 mM Cu(II) ion concentration; [d] form Ref. [43]; [e] at 25 °C and 20 MHz.

## Experimental section

### Synthesis

All commercially purchased reagents (Sigma-Aldrich) and solvents (Scharlab) were used as received and without further purification. NMR spectra were acquired on Bruker Avance 360 and 400 MHz spectrometers and processed/analyzed using MestreNova 8.1 (Mestrelab Research) or Topspin (Bruker) softwares. The ESI QTOF (Electro Spray Ionization Quadrupole Time of Flight) spectrometry was performed at the Department of Applied Chemistry of the University of Debrecen.

**a). Synthesis of *cis*-1,2-CDTA-tetraethyl ester:** Ethyl-bromoacetate (6.14 g, 36.8 mmol, 4.2 equiv.) was dissolved in dry acetonitrile and added dropwise to the mixture of 1.00 g (8.76 mmol) *cis*-1,2-diaminocyclohexane, 5.66 g N,N-diisopropylethylamine (43.8 mmol, 5.0 equiv.) and 1.31 g (8.76 mmol, 1.0 equiv.) of NaI prepared in dry acetonitrile (30 ml). The reaction mixture was then heated to reflux in $N_2$ atmosphere and kept at this temperature for 7 hours. The precipitate formed in the course of reaction was filtered off from the hot solution and the filtrate was evaporated under reduced pressure. The resulting oily residue was dissolved in 40 mL of bi-distilled water and extracted with portions of chloroform (3×40 mL). The combined organic fraction was dried over anhydrous $Na_2SO_4$ and evaporated under

21

reduced pressure. The purification of the title product by flash chromatography on silica gel by using petrolether and ethyl acetate (increasing the ethyl acetate content of the eluent gradually form 10:1 to 5:1 by volume) yielded the pure substance (0.82 g which corresponds to 20 % yield). $R_f$ in 5:1 petrolether : ethyl acetate is 0.38.

^{1}H-NMR: (360.13 MHz, CDCl₃): δ = 1.23 (12H, t, $J$ = 7.11 Hz, -O-CH₂-**CH₃**); 1,29 (2H, m, -**CH₂**-); 1.43 (2H, m, -**CH₂**-); 1.62 (2H, m, -**CH₂**-); 1.79 (2H, m, -**CH₂**-); 3.16 (2H, d, $J$ = 6.88 Hz, -C**H**-); 3.70 and 3.79 (8H, AB doublet, $^2J_{AB}$ = 17.90 Hz, -N-**CH₂**-COO-); 4.11 (8H, q, $J$ = 7.11 Hz, -O-**CH₂**-CH₃). ^{13}C-NMR: (90.55 MHz, CDCl₃): δ = 14.34 (4C, s, -O-CH₂-**CH₃**); 23.44 (2C, s, -**CH₂**-CH₂-); 26.88 (2C, s, -**CH₂**-); 53.08 (4C, s, -N-**CH₂**-COO-); 60.27 (4C, s, -O-**CH₂**-CH₃); 60.55 (2C, s, -**CH**-); 172.58 (-N-CH₂-**C**OO-). MS (ESI-Q-TOF): $m/z$ [M+] calculated for $C_{22}H_{38}N_2ONa$: 481.252; found: 481.251

**b). Synthesis of *cis*-1,2-CDTA:** 0.40 g NaOH (10 mmol, 6 equiv.) was dissolved in 1,0 mL of bi-distilled water and was added portionwise to the solution of 0.75 g (1.64 mmol) *cis*-1,2-CDTA-tetraethyl ester dissolved in 15 mL of ethanol. The reaction mixture was heated to 78 ◦C and refluxed at this temperature for 24 h. The white precipitate formed during the reaction (Na₄(c-cdta)) in the reaction mixture was filtered off and washed twice with cold ethanol (2×10 mL), diethyl ether (2×10 mL) and dried to constant weight. The solid obtained was dissolved in minimal amount of water required to dissolve it (3.0 mL) and pH of the sample was set to pH=2.02 by addition of concentrated HCl. The white precipitate formed as a result of acid addition was filtered off and washed with small portions of acidified distilled water (pH=2.50), cold ethanol (2×5 mL), diethyl ether (2×5 mL) and dried until the weight of the product become constant. Yield: 0.22 g (39 %).

^{1}H-NMR: (360.13 MHz, D₂O): δ = 1,51 (2H, m, -**CH₂**-); 1.74 (2H, m, -C**H₂**-); 1.83 (2H, m, -**CH₂**-); 2.00 (2H, m, -**CH₂**-); 3.51 (2H, m, -C**H**-); 3.83 and 4.01 (8H, AB doublet, $^2J_{AB}$ = 17.39 Hz, -N-C**H₂**-COO-). ^{13}C-NMR: (90.55 MHz, D₂O): δ = 22.11 (2C, s, -**CH₂**-CH₂-); 23.19 (2C, s, -**CH₂**-); 54.76 (4C, s, -N-C**H₂**-COO-); 61.26 (2C, s, -**CH**-); 172.81 (-N-CH₂-**C**OO-). MS (ESI-Q-TOF): $m/z$ [M+] calculated for $C_{14}H_{21}N_2O_8NaNa$: 391.109; found: 391.109

**Equilibrium studies**

The chemicals ($MCl_2$ salts) used in the studies were of the highest analytical grade. The concentration of the stock solutions was determined by complexometric titration using a

22

standardized $Na_2H_2edta$ solution and appropriate indicators (Patton & Reeder ($CaCl_2$), Eriochrome Black T ($MgCl_2$ and $MnCl_2$), xylenol orange ($ZnCl_2$), murexid ($CuCl_2$)) [49]. The pH-potentiometric titrations were carried out with a Methrohm 888 Titrando titration workstation, using a Metrohm 6.0233.100 combined electrode. The titrated solutions (6.00 mL) were thermostated at 25 °C. The samples were stirred and kept under inert gas atmosphere ($N_2$) to avoid the effect of $CO_2$. The calibration of the electrode was performed by two point calibration (KH-phthalate (pH = 4.005) and borax (pH = 9.177) buffers). The calculation of [$H^+$] from the measured pH values was performed with the use of the method proposed by Irving *et al.* [50] by titrating a 0.01 M HCl solution ($I$ = 0.15 M NaCl) with a standardized NaOH solution. The differences between the measured ($pH_{read}$) and calculated pH (-log [$H^+$]) values were used to obtain the equilibrium $H^+$ concentrations from the pH-data obtained in the titrations. The ion product of water was determined from the same experiment in the pH range 11.4 – 12.0.

The concentration of the *c*-cdta ligand was determined by pH-potentiometric titration, comparing the titration curves obtained in the presence and absence of moderate Mn(II) excess. The protonation constants of *c*-cdta as well as the stability and protonation constants of the complexes formed with Mg(II) Ca(II), Mn(II), Cu(II) and Zn(II) were also determined by pH-potentiometric titration. The metal-to-ligand concentration ratio was 1:1 (the concentration of the ligand was generally 2.50 − 3.00 mM). The pH-potentiometric titrations curves were measured in the pH range 1.8 − 11.8 and 44 − 205 mL NaOH–pH data pairs were collected and fitted.

The stability constant and solution speciation of the [Mn(*c*-cdta)]$^{2−}$ complex was confirmed using $^1H$ relaxometry in order to support the stability constant value obtained by pH-potentiometry (for details about $T_1$ measurements, see the "Relaxivity determination" section below). 3.00 mL of a 1.02 mM [Mn(*c*-cdta)]$^{2−}$ sample were titrated with solid NaOH or gasous HCl (in order to avoid sample dilution) to adjust the pH in the range 1.97 − 7.12, followed by recording and averaging of 5 − 6 $T_1$ values for each pH data point.

Owing to the high conditional stability of [Cu(*c*-cdta)]$^{2-}$, the formation of the complex was complete (nearly 100%) even at pH = 1.54 (starting point of the pH-potentiometric titration). For this reason, 12 out-of-cell (batch) samples containing a slight excess of ligand and the Cu(II) ion were prepared ($c_L$ = 3.528 mM, $c_{Cu2+}$ = 3.410 mM, 25 °C, 0.5 M ($Na^+$+$H^+$)$Cl^-$). The samples, whose acidity was varied in the concentration range of 12.1 − 462 mM, were equilibrated for 1 day before recording the absorption spectra at 25 °C in Peltier

thermostated semi-micro 1 cm Hellma® cells using a Varian CARY 1E, UV-Vis spectrophotometer. The molar absorptivity of the $[Cu(c\text{-cdta})]^{2-}$, complex was determined at 21 wavelengths (600 − 800 nm range) by recording the spectra of $1.72 \times 10^{-3}$, $2.55 \times 10^{-3}$ and $3.48 \times 10^{-3}$ M complex solutions, while for the Cu(II) ion, previously published molar absorptivity values (determined under identical conditions) [51] were used for the data fitting. The molar absorption coefficients of monoprotonated $[CuH(c\text{-cdta})]^{2-}$ were calculated during the simultaneous data refinement (UV-vis and pH-potentiometric titration curves). The protonation (ligand and complexes) and stability constants (complexes) were calculated from the titration data with the PSEQUAD program [52].

**Kinetic studies**

The dissociation rates of the $[Mn(c\text{-cdta})]^{2-}$ chelate were studied at 25 $^{\circ}$C (Peltier thermostated) and 0.15 M NaCl ionic strength by stopped-flow method monitoring the formation of the Cu(II) complex at 300 nm using an Applied Photophysics DX-17MV instrument. All dissociation reactions were performed under pseudo-first order conditions where the exchanging metal ion (Cu(II)) was in 10–40-fold excess relative to the complex ($c_{complex} = 2.0 \times 10^{-4}$ M, pH range 4.25–5.10). The kinetic studies were carried out in a non-coordinating buffer to maintain the pH in the samples constant (0.05 M $N$,-methylpiperazine (nmp) with log $K_2^H = 4.34$ under the conditions applied). The pseudo-first-order rate constants ($k_{obs}$) were calculated by fitting the absorbance-time data series to equation 9:

$$A_t = (A_0 - A_e)e^{-k_{obs}t} + A_e \qquad \text{(eqn. 9)}$$

where $A_t$, $A_0$ and $A_e$ are the absorbance at time t, at the start and at the equilibrium of the reaction, respectively. The calculations were performed with the computer program Micromath Scientist, version 2.0 (Salt Lake City, UT, USA) by using a standard least-squares procedure [53].

**$^1$H-, and $^{17}$O-NMR relaxometry**

Longitudinal ($1/T_1$) and transverse ($1/T_2$) relaxation rates and chemical shifts of an aqueous solution of the Mn(II) complex (pH=7.4, 10.3 mM) and of a diamagnetic reference (HClO$_4$ acidified water, pH = 3.3) were measured in the temperature range 273 − 338 K using a Bruker Avance 400 (9.4 T, 54.2 MHz) spectrometer. The temperature was determined according to previous calibration by means of ethylene glycol and methanol as standards [54].

24

$1/T_1$ and $1/T_2$ values were determined by the inversion - recovery and the Carr − Purcell − Meiboom −Gill spin − echo technique, respectively [55]. The technique of the ^{17}O NMR measurements has been described previously [56]. To avoid susceptibility corrections of the chemical shifts, a glass sphere fitted into an 10 mm NMR tube was used to contain the samples. To improve sensitivity, [17]O enriched water (10% $H_2^{17}O$, CortecNet) was added to the solutions to reach around 1% enrichment.

Proton NMRD profiles of the $[Mn(c\text{-cdta})]^{2-}$ complex (1.00 mM, pH = 7.4) were recorded in aqueous solution on a Stelar SMARTracer Fast Field Cycling relaxometer (0.01 − 10 MHz) and a Bruker WP80 NMR electromagnet adapted to variable field measurements (20 − 80 MHz) and controlled by a SMARTracer PC-NMR console. The temperature was monitored by a VTC91 temperature control unit and maintained by a gas flow. The temperature was determined by previous calibration with a Pt resistance temperature probe. The least-squares fit of the ^{17}O NMR and of the NMRD data was performed using Visualiseur/Optimiseur [57, 58] running on a MATLAB 8.3.0 (R2014a) platform.

### Relaxivity determination

The longitudinal water proton relaxation rate ($r_1 = 1/T_1 - 1/T_w$) was measured at 20 MHz with a Bruker Minispec MQ-20 relaxometer (Bruker Biospin, Germany). Samples were thermostated by using a circulating water bath at $25.0 \pm 0.2$ °C. The longitudinal relaxation times ($T_1$) were measured by using the inversion recovery method ($180° − \tau − 90°$) by averaging 5 − 6 data points for each concentration point obtained by using 14 different $\tau$ values ($\tau$ values ranging between 0 to at least 6 times the expected $T_1$).

### DFT calculations

The $[Mn(c\text{-cdta})(H_2O)]^{2-} \cdot 2H_2O$ and $[Mn(t\text{-cdta})(H_2O)]^{2-} \cdot 2H_2O$ systems were fully optimized by using the hybrid meta-GGA M062X functional and the TZVP basis set [59, 60]. The nature of optimized geometries as true energy minima was confirmed by frequency analysis. Frequency calculations provided zero-point energies (ZPEs), enthalpies (*H*) and free energies (*G*) at 298.15 K and 1 atm. The relative free energies include non-potential-energy contributions (zero point energies and thermal terms) obtained through frequency analysis. Hyperfine coupling constants were calculated on the optimized structures by using the EPR-III basis set for the ligand atoms and the aug-cc-pVTZ-J basis set for Mn [61, 62].

Throughout this study bulk solvent effects were considered by using the integral equation formalism variant of the polarizable continuum model (IEFPCM) [63].

**Abbreviations**

| | |
|---|---|
| MRI | Magnetic resonance imaging |
| DFT | Density Functional Theory |
| APC | aminopolycarboxylate |
| CA | Contrast Agent |
| dtpa | Diethylenetriaminepentaacetic acid |
| dota | 1,4,7,10-Tetraazacyclododecane-1,4,7,10-tetraacetic acid |
| NSF | Nephrogenic Systemic Fibrosis |
| edta | Ethylenediaminetetraacetic acid |
| *trans*-1,2-cdta | *trans*-1,2-Diaminocyclohexane-N,N,N′,N′-tetraacetic acid |
| *cis*-1,2-cdta | *cis*-1,2-Diaminocyclohexane-N,N,N′,N′-tetraacetic acid |
| dipea | N,N-diisopropylethylamine |
| ida | Iminodiacetate |
| NMRD | Nuclear magnetic relaxation dispersion |
| 4-het-cdta | 4-((1-(2-Hydroxyethyl)-1H[1,2,3]triazol-4-yl)methoxy)methyl-trans-1,2-diaminocyclohexane-N,N,N',N'-tetraacetic acid |
| 1,4-do2a | 1,4,7,10-Tetraazacyclododecane-1,4-diacetic acid |
| do1a | 1,4,7,10-Tetraazacyclododecane-1-acetic acid |
| phdta | *o*-Phenylenediamine tetraacetate |
| ESI QTOF | Electro Spray Ionization Quadrupole Time of Flight |
| nmp | *N*-methylpiperazine |

26

ZPEs          Zero-point energies

## Appendix A. Supplementary data

Supplementary data associated with this article ($^1$H-, $^{13}$C-NMR and MS data of the pure compounds, comparison of X-ray and DFT structures and the equations related to the solvent exchange kinetics data refinement) can be found, in the online version, at http://dx.doi.org/10.1016/xxxxxxxxxxxxxxxxx .

## Acknowledgements

## References

[1] Anderson L. J., Welch M. J., Chem. Rev. 1999, 99(9), 2219-34.

[2] Stimmel J.B., Kull F.C. Jr., Nucl. Med. Biol. 1998, 25, 117-125.

[3] Nayak T. K., Brechbiel M. W., Bioconjug. Chem. 2009, 20(5), 825-841.

[4] Parker D., Dickins R. S., Puschmann H., Crossland C. and Howard J. A. K., Chem. Rev. 2002, 102 (6), 1977-2010.

[5] Montgomery C. P., Murray B. S., New E. J., Pal R., Parker D., Acc. Chem. Res., 2009, 42 (7), 925-937.

[6] Caravan P., Ellison J. J., McMurry T. J., Lauffer R. B., Chem. Rev. 1999, 99(9), 2293-2352.

[7] The Chemistry of Contrast Agents in Medical Magnetic Resonance Imaging, 2$^{nd}$ edition, Eds. Merbach A. E, Helm L. Tóth É., John Wiley and Sons, London, 2013.

[8] Grobner T., Nephrol. Dial. Transplant. 2006, 21, 1104-1108.

[9] Marckmann P., Skov L., Rossen K., Dupont A., Damholt M. B., Heaf J. G., Thomsen H. S., J. Am. Soc. Nephrol. 2006, 17, 2359-2362.

[10] Kitajima K., Maeda T., Watanabe S., Ueno Y., Sugimura K., Int. J. Urol. 2012, 19, 806-811.

[11] Kanda T., Fukusato T., Matsuda M., Toyoda K., Oba H., Kotoku J., Haruyama T., Kitajima K., Furui S., Radiology 2015, 276, 228-232.

[12] Kanal E., Tweedle, M. F., Radiology 2015, 275, 630-634.

[13] Roberts D. R., Lindhorst S. M., Welsh C. T., Maravilla K. R., Herring M. N., Braun K. A., Thiers B. H., Davis W. C., Invest Radiol. 2016, 51(5), 280-289.

[14] Birka M., Wentker K. S., Lusmöller E., Arheilger B., Wehe C. A., Sperling M., Stadler R., Karst U., Anal. Chem. 2015, 87(6), 3321-8.

[15] Troughton J. S., Greenfield M. T., Greenwood J. M., Dumas S., Wiethoff A. J., Wang J., Spiller M., McMurry T. J., Caravan P. Inorg. Chem., 2004, 43(20), 6313-23

[16] Wang S., Westmoreland D. T., Inorg. Chem. 2009, 48(2), 719-27.

[17] Drahoš B., Kubíček V., Bonnet C. S., Hermann P., Lukeš I, Tóth É., Dalton Trans. 2011, 40(9), 1945-51.

[18] Kálmán F. K., Tircsó Gy., Inorg. Chem. 2012, 51(19), 10065-17.

[19] Drahos B., Kotek J., Hermann P., Lukes I., Tóth É., Inorg. Chem. 2010, 49, 3224-38.

[20]    Tei L., Gugliotta G., Fekete M., Kálmán F. K., Botta M., Dalton Trans. 2011, 40(9), 2025-32

[21]    Regueiro-Figueroa M., Rolla G. A., Esteban-Gómez D., de Blas A., Rodríguez-Blas T., Botta M., Platas-Iglesias C., Chem. Eur. J. 2014, 52(20), 17300–17305.

[22]    Gale E. M., Atanasova I. P., Blasi F., Ay I., Caravan P., J. Am. Chem. Soc. 2015, 137, 15548-15557.

[23]    Forgács A., Pujales-Paradela R., Regueiro-Figueroa M., Valencia L., Esteban-Gómez D., Botta M., Platas-Iglesias C., Dalton Trans. 2017, 46, 1546-1558.

[24]    Phukan B., Patel A. B., Mukherjee C., Dalton Trans. 2015, 44, 12990-12994.

[25]    Ussov W.Y., Beljanin M.L. Borodin O.Y., Churin A.A., Bezlepkin A.I., Filimonov V.D., Medical Visualization (in russian) 2009, 5 121-132.

[26]    Ussov W.Y., Bogunetsky A.A., Babokin V.E., Belyanin M.L., Goltsov S.G., Filimonov V.D., Tomsk/RU In ECR, 2014 March 6–10, 2014, Vienna, Austria; B-0904.

[27]    Critical Stability Constants, Ed. Martell A. E., Smith R. M., Vol. 1-6. Plenum Press, New York, London, 1974-1989.

[28]    Charlier L., Merciny E., Fuger, J., Anal. Chim. Acta, 1985, 178, 299-306.

[29]    Drahoš B., Kotek J., Hermann P., Lukeš I., Tóth É., Inorg. Chem. 2010, 49(7), 3224-3238

[30]    Sudmeier J. L., Reilley C. N., Anal. Chem. 1964, 36(9), 1707-712.

[31]    Regueiro-Figueroa M., Ruscsák E., Fra L., Tircsó Gy., Tóth I., de Blas A., Rodríguez-Blas T., Platas-Iglesias C. and Esteban-Gómez D., Eur. J. Inorg. Chem. 2014, 36, 6165-6173.

[32]    Rodríguez-Rodríguez A., Garda Z., Ruscsák E., Esteban-Gómez D., de Blas A., Rodríguez-Blas T., Lima L. M. P., Beyler M., Tripier R., Tircsó Gy.. Platas-Iglesias C., Dalton Trans., 2015,44, 5017-5031.

[33]    Thakral C., Abraham J.L., J. Cutan Pathol. 2009, 36(12),1244-54.

[34]    Port M., Idée J.M., Medina C., Robic C., Sabatou M., Corot C., Biometals. 2008, 21(4), 469-90.

[35]    Smith G. F., Margerum D. W, Inorg. Chem. 1969, 8(1), 135-138.

[36]    Margerum D. W., JPausch. B., Nyssen G. A., Smith G. F., Anal. Chem. 1969, 41(2), 233-238.

[37]    Gale E. M., Zhu J., Caravan P. J. Am. Chem. Soc. 2013, 135(49), 18600-18608.

[38]    Bloembergen N.; Morgan L. O., J. Chem. Phys. 1961, 34, 842-850.

[39]    Freed J. H., J.Chem.Phys. 1978, 68, 4034-4037.

[40]    Swift T. J., Connick R. E., J.Chem.Phys. 1962, 37, 307-320.

[41]    Swift T. J., Connick R. E., J.Chem.Phys. 1964, 41, 2553-2554.

[42]    Maguit J., Meier R., Zahl A., Eldik R., Inorg. Chem. 2008, 47, 5702-5719.

[43]    Vanasschen C., Molnár E., Tircsó Gy., Kálmán F. K., Tóth É., Brandt M., Coenen H. H., Neumaier B., Inorg. Chem., 2017, 56(14), 7746–7760.

[44]    Ruloff R., Tóth É., Scopelliti R., Tripier R., Handle H., Merbach A. E., Chem. Commun. 2002, 22, 2630-2631.

[45]    Esteban-Gomez D., Cassino C., Botta M., Platas-Iglesias C., RSC Advances 2014, 4, 7094-7103.

[46]    Rolla G. A., Platas-Iglesias C., Botta M., Tei L., Helm L., Inorg. Chem., 2013, 52, 3268-3279.

[47]    Patinec, V., Rolla, G. A., Botta, M., Tripier, R., Esteban-Gómez, D., Platas-Iglesias, C., Inorg. Chem. 2013, 52, 11173-11184.

[48]    Wang, X. F., Gao, J., Wang, J., Zhang, Z. H., Wang, Y. F., Chen, L. J., Sun, W., Zhang, X. D., J. Struct. Chem., 2008, 49, 724-731

[49]    Schwarzenbach G., Flaschka H. A., Complexometric titrations. Barnes & Noble: 1969.

[50]    Irving H. M., Miles M. G., Pettit L. D., Anal. Chim. Acta 1967, 38, 475-488.

[51]    Molnár E., Camus N., Patinec V., Rolla G. A., Botta M., Tircsó Gy., Kálmán F. K., Fodor T., Tripier R., Platas-Iglesias C., Inorg. Chem. 2014, 53 (10), 5136-5149.

[52]    Zékány, L.; Nagypál, I., PSEQUAD. In Computational Methods for the Determination of Formation Constants, Leggett, D. J., Ed. Springer US: Boston, MA, 1985; pp 291-353.

[53]    https://www.micromath.com/ (last accessed on 19th of July, 2017).

[54]    Raiford D. S., Fisk C. L., Becker E. D., Anal. Chem. 1979, 51, 2050-51.

[55]    Meiboom S., Gill D., Rev. Sci. Instrum. 1958, 29, 688-691.

[56]    Micskei K., Helm L., Brucher E., Merbach A. E., Inorg. Chem., 1993, 32, 3844-3850.

[57]    Yerly F., VISUALISEUR 3.3.7; Lausanne, Switzerland, 2006.

[58]    Yerly F., OPTIMISEUR 3.3.7. Lausanne, Switzerland, 2006.

[59]    Zhao, Y., Truhlar, D. G., Theor. Chem. Acc., 2008, 120, 215-241.

[60]    Schäfer, A., Huber, C., Ahlrichs, R., J. Chem. Phys., 1994, 100, 5829-5835.

[61]    Rega, N., Cossi, M., Barone, V., J. Chem. Phys., 1996, 105, 11060-11067.

[62]    Hedegard, E. D., Kongsted, J., Sauer, S. P. A., J. Chem. Theory Comput., 2011, 7, 4077-4087.

[63]    Tomasi, J., Mennucci, B., Cammi, R. Chem. Rev., 2005, 105, 2999-3093.

**Highlights**

- Stability constants, water exchange rates and the relaxivities of the isomeric $[Mn(cdta)]^{2-}$ complexes are similar

-The conditional stability and the inertness of the $[Mn(t\text{-cdta})]^{2-}$ is higher than that of $[Mn(c\text{-cdta})]^{2-}$

-The *trans*-1,2-cyclohexanediamine unit is an excellent "building block" when designing Mn(II) complexes as safe MRI agents

**TOC graphic**
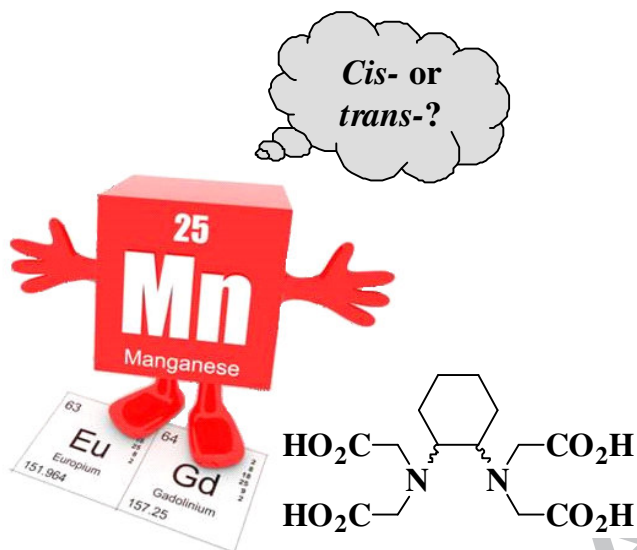


M(II) complexes formed with *c*-cdta (*cis*-1,2-diaminocyclohexane-*N,N,N',N'*-tetraacetic acid) chelator have been investigated by pH-potentiometry, UV-vis spectrophotometry, $^1$H and $^{17}$O NMR relaxometry. pMn as well as the inertness of the Mn(II) complex formed with *c*-cdta ligand were found to differ substantially form those found for the *trans*- derivative while the water exchange rate and the relaxivity do not differ remarkably. Our results confirm, that the *t*-cdta platform has better potential for further ligand development owing to better dissociation kinetic parameters of its Mn(II) complex.